

Modelamiento y simulación de susceptibilidad magnética AC en manganitas $\text{La}_{2/3}\text{Ca}_{1/3}\text{MnO}_3$

Modeling and simulation of AC magnetic susceptibility in $\text{La}_{2/3}\text{Ca}_{1/3}\text{MnO}_3$ manganites

^{1,2}Hector Barco Ríos, ¹Edilberto Rojas Calderón, ²Elisabeth Restrepo-Parra.

¹PCM Computational Applications, Universidad Nacional de Colombia Sede Manizales, Colombia

²Departamento de Física y Química, Universidad Nacional de Colombia Sede Manizales, Colombia

Correo-e: erestrepopa@unal.edu.co

Resumen— En este trabajo se propone un modelo para obtener la susceptibilidad magnética AC de manganitas $\text{La}_{2/3}\text{Ca}_{1/3}\text{MnO}_3$. Las muestras están compuestas por una combinación de iones Mn^{4+} y Mn^{3+} que influyen la estequiometría del material. El modelo se basa en un Hamiltoniano que incluye interacción Heisenberg y efecto Zeeman. Para determinar la susceptibilidad AC, se aplica un campo magnético externo dependiente del tiempo $h(t)$ a la muestra. Para llevar a cabo las simulaciones se requirieron algunas herramientas matemáticas, tales como transformadas de Fourier. El estudio fue llevado a cabo para diversas frecuencias angulares y temperaturas. Las simulaciones se obtuvieron empleando una interfaz gráfica que permitió el monitoreo en línea de los resultados. De acuerdo con dichos resultados, la susceptibilidad AC disminuye no solo con la temperatura, sino también con la frecuencia.

Palabras clave— Monte Carlo, transformada de Fourier, dependencia del tiempo, susceptibilidad AC.

Abstract— In this study, a model for obtaining the AC magnetic susceptibility of $\text{La}_{2/3}\text{Ca}_{1/3}\text{MnO}_3$ manganites was proposed. The samples were composed of a combination of Mn^{4+} and Mn^{3+} ions that influence the material stoichiometry. The model is based on the Hamiltonian, including the Heisenberg interaction and the Zeeman effect. For determining AC susceptibility, a time-dependent external magnetic field $h(t)$ was applied to the sample. Several mathematical tools, such as Fourier transforms, were required for performing the simulations. The study was conducted for various angular frequencies and temperatures. The simulations were obtained using a graphic interface that allowed the online monitoring of the results. According to the results, the AC susceptibility decreases not only with the temperature, but also with the frequency.

Key Word — Coercive field, critical temperature, Magnetic properties, Monte Carlo.

I. INTRODUCTION

Recently, perovskite-type manganites with formula $\text{Ln}_{1-x}\text{A}_x\text{MnO}_3$ (being Ln and A, a large lanthanide and an alkaline-earth respectively) have attracted considerable interest after the discovery of CMR (colossal magneto resistance) properties in certain of these materials. Moreover, research on CMR materials has enabled understanding of the fundamental aspects of the physics of highly correlated electron systems, such as manganites [1]. These materials present interesting electrical properties, exhibiting a maximum at a certain temperature T_{MI} corresponding to a metal-insulator transition. This transition is drastically suppressed by application of a magnetic field [2]. Another important characteristic of these materials is a ferromagnetic-paramagnetic transition at a temperature T_C near T_{MI} [3]. Several parameters influence the physical properties of these materials. Two of the most meaningful parameters are the density of carriers represented by the $\text{Mn}^{4+}/\text{Mn}^{3+}$ ratio [4,5] and the Mn-O-Mn bond angle that has a strong influence on the orbital overlapping between neighboring ions [6]. In the literature, there are several reports that present experimental studies of DC magnetic properties in LCMO compounds, such as magnetization, DC susceptibility and magnetoresistance [7-9]. AC magnetic susceptibility measurements have been widely used for characterizing the magnetic transitions that occur in several materials [10,11]. Frequently, the behavior of the AC susceptibility can be attributed to either an intrinsic spin glass behavior or to extrinsic phenomena, such as domain wall pinning [12]. The presence of these complex mechanisms can hamper efforts to analyze the AC magnetic response. A comprehensive review of the theoretical and experimental aspects relative to the origin of the phase transition and its field dependence has been conducted by Williams [13] based on the classical framework of a second order paramagnetic/ferromagnetic transition theory. This

phase transition has been experimentally determined in dilute magnetic systems, such as AuFe [14], PdMn [15] and amorphous ferromagnetic alloys [16]. Moreover, similar behavior was also observed in manganites, such as $\text{La}_{0.67}\text{Pb}_{0.33}\text{MnO}_3$ [17], $\text{La}_{0.67}\text{Ca}_{0.33}\text{MnO}_3$ [18] and $\text{La}_{1-x}\text{Mg}_x\text{MnO}_3$ [19-20].

With respect to theoretical studies and simulations, in the literature, it is common to find reports presenting results for DC magnetization and magnetic susceptibility using methods, such as Monte Carlo [21-23]. Nevertheless, few reports can be observed presenting simulations of AC magnetic susceptibility. It is possible that this absence is due to the complexity and the computational cost that these simulations require.

In the present work, AC magnetic susceptibility simulations of $\text{La}_{2/3}\text{Ca}_{1/3}\text{MnO}_3$ using a Monte Carlo method are reported and discussed. The AC susceptibility was derived from the magnetization, depending on the time and later application of a Fourier transform, for obtaining its dependence on frequency. Finally, the influence of the temperature was evaluated.

II. METODOLOGY

Manganite $\text{La}_{2/3}\text{Ca}_{1/3}\text{MnO}_3$ crystallizes in a perovskite structure in which trivalent Mn^{3+} and tetravalent Mn^{4+} ions are distributed into the lattice, thereby forming a simple cubic array. This structure was widely considered to be true, even though there are reports indicating that the electronic structure of the surface is, in general, notably different from the bulk, forming a pseudo-cubic structure [24]. In addition, the manganite structure has been investigated by E. O. Wollan and W. E. Koehler [25]. In a simulation model, magnetic Mn^{3+} and Mn^{4+} ions are represented by Heisenberg spins, while oxygen, lanthanum and calcium ions are considered to be non-magnetic. The Heisenberg Hamiltonian describing the system reads as follows [26]:

$$H = - \sum_{i=0}^N \sum_{j \neq i}^N J_{ij} \vec{S}_i \cdot \vec{S}_j - \vec{h}(t) \sum_{i=0}^N \vec{S}_i \quad (1)$$

where N is the number of atomic positions in the sample. The first sum includes the nearest magnetic neighbors, whereas $|\vec{S}_i|$ and $|\vec{S}_j|$ take values of 2 for $\text{Mn}^{3+\text{eg}}$ and $\text{Mn}^{3+\text{eg}'}$ or $3/2$ for $\text{Mn}^{4+\text{d}3}$ based upon the electronic configurations of these ions. In addition, the spins interact via ferromagnetic superexchange interactions for Mn^{3+} - Mn^{3+} (e_g - e_g), Mn^{3+} - Mn^{4+} (e_g - d_3) and Mn^{3+} - Mn^{4+} (e_g - d_3) [20]. Numerical values for the superexchange integrals were considered according to the orbital order pattern as reported by T. Hotta et al. [27]. Three types of bonds are considered: $\text{Mn}^{3+\text{eg}'}$ - O - $\text{Mn}^{3+\text{eg}}$ ($J_{ij}=7.77$ meV), $\text{Mn}^{3+\text{eg}}$ - O - $\text{Mn}^{4+\text{d}3}$ ($J_{ij}=3.66$ meV) and $\text{Mn}^{3+\text{eg}'}$ - O - $\text{Mn}^{4+\text{d}3}$ ($J_{ij}=4.65$ meV); these values have been reported previously [28]. A single-spin movement Metropolis Monte Carlo algorithm was used for obtaining equilibrium thermodynamic properties [29]. The

second term corresponds to the influence of the external magnetic field, which depends on the time according to the following expression:

$$h(t) = h_{\max} \cos(\omega t + \varphi) \quad (2)$$

where h_{\max} is the maximum value of the magnetic field ($h_{\max}=1.35$ Oe), $\omega=2\pi f$ is the angular frequency, with $f=20$ Hz, 80 Hz, 100 Hz, 300 Hz and 1000 Hz, $\varphi=0$. Periodic boundary conditions in the transverse directions and free along the perpendicular direction of the film were employed. A linear dimension $L=12$ (in lattice parameters units) along the x - y plane and several thicknesses d in the z direction were used. In the vicinity of the critical region, the temperature step was 0.005 K. In computing equilibrium averages, approximately 1×10^4 Monte Carlo steps per spin (mcs) were considered after equilibration. The procedure was the following: (i) initially, the magnetization was obtained as a function of time (t) and for each temperature (T). The magnetization can be obtained as a function of time t and temperature T using the next equation

$$M(t, T) = \frac{1}{N} \sum_{i=1}^N \vec{S}_i \quad (3)$$

After obtaining the magnetization depending on the time, for each frequency ω during the cycle, and for a given temperature T , the AC magnetic susceptibility $\chi(t, T)$ can be written as follows [30]:

$$\chi(t, T) = \frac{M(t, T)}{h(t)} \quad (4)$$

In this equation, $h(t)$ is the external magnetic field applied to the sample according to equation 2. Next, the values of $\chi(t, T)$ can be determined for each cycle, depending on the time, t , at different temperatures. To explain the procedure for obtaining the ac AC susceptibility, the curve for $T=150$ K was chosen. From these curves, a function that can fit this behavior was obtained as follows:

$$\chi(t, T) = (a + bt + ct^2)^{-1} \quad (5)$$

for each temperature, where a , b and c , are parameters for the curve fitting. The AC magnetic susceptibility can be written in terms of a Fourier series [31]:

$$\chi(t, T) = \sum_{n=1}^{\infty} \left[\chi_n' \cos(n\omega t) + \chi_n'' \sin(n\omega t) \right] \quad (6)$$

In this equation, the Fourier expansion coefficients χ_n' and χ_n'' correspond to the real and imaginary components of AC susceptibility, respectively, where n is an integer. The two first terms of the Fourier series were chosen because they are the most representative, while the others can be

neglected. For determining these coefficients, a Fourier transformation was used. The next expressions were used:

$$\chi'_n = \frac{2}{T} \int_0^T \chi(t, T) \cos(n\omega t) dt \quad (7)$$

$$\chi''_n = \frac{2}{T} \int_0^T \chi(t, T) \sin(n\omega t) dt \quad (8)$$

For evaluating these integrals and determining the real and imaginary components of the AC susceptibility, equation (5) is used in (7) and (8); next, these integrals are solved by means of a Monte Carlo method. This procedure is conducted for each temperature.

Summarizing the steps for carrying out the simulations: (i) samples of $\text{La}_{2/3}\text{Ca}_{1/3}\text{MnO}_3$ are built according to the procedure described above; (ii) the model of eq. (1) is applied to the system for obtaining the magnetization based on eq. (3) and the susceptibility based on eq. (4), using the Monte Carlo method and the Metropolis algorithm, where the external magnetic field is represented by eq. (2), with the frequency and the temperature being remained constant and the time (t) being variable; (iii) the susceptibility curve was fitted using eq. (5) to obtain the values of a , b and c ; (iv) once the equation was obtained, the real and imaginary components of the AC susceptibility were obtained by applying eq. (7) and (8); (v) After this procedure, the value of the temperature was changed (with a step of 2 K), while holding the frequency constant; (vi) once the temperature was varied between 100 and 300 K, the frequency was changed and was later remained constant, while the temperature was scanned; finally, (vii) this procedure was repeated until all of the frequencies were simulated

III. RESULTS AND DISCUSSION

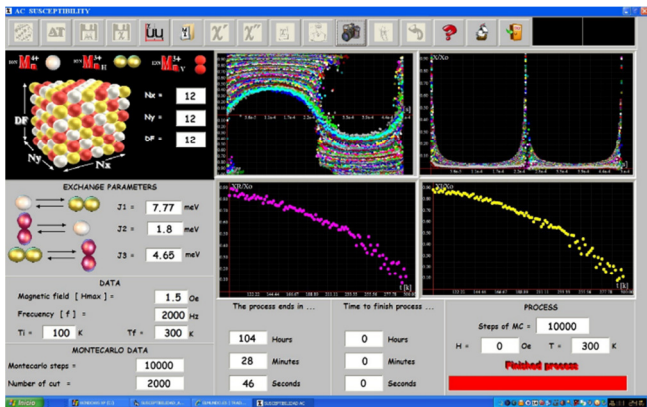


Figure 1. Graphical interface built for obtaining the AC magnetic properties.

Figure 1 shows the user graphical interface used for obtaining the AC susceptibility. Using this graphical interface, values of the parameters employed in the simulations are introduced. This graphical interface was built using Visual Basic. The upper component contains several buttons that enable the process to be conducted, such

as data capture, save, clean, help and exit. At the upper left corner, the sample construction is observed with its corresponding geometry and configuration. The lower left panel contains data input, such as exchange parameters, temperature, magnetic field and number of Monte Carlo steps. The upper right panel contains boxes presenting the graphic resulting from the simulations. The lower right panel shows the time that the simulation will take and the number of Monte Carlo steps that have been completed.

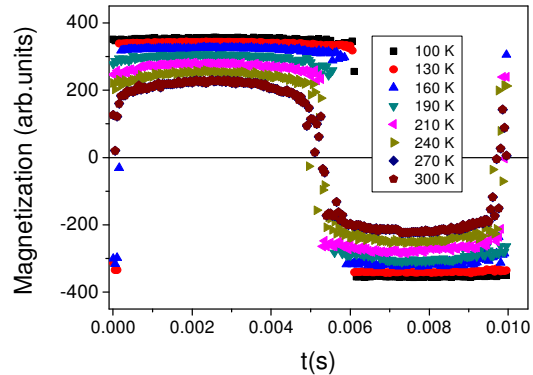


Figure 2. Magnetization as a function of time (t) for $\text{La}_{2/3}\text{Ca}_{1/3}\text{MnO}_3$ manganites at several temperatures, $f=20$ Hz and $H_{max}=1.35$.

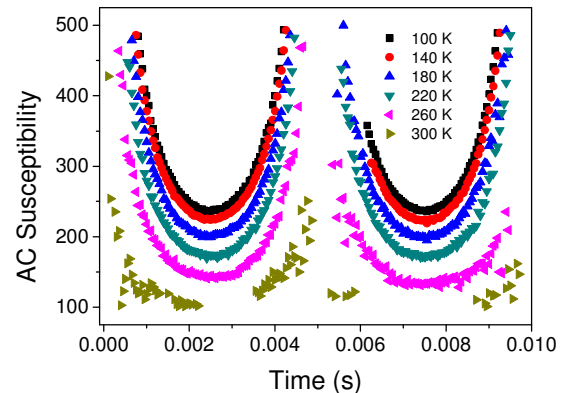


Figure 3. AC susceptibility as a function of time (t) for $\text{La}_{2/3}\text{Ca}_{1/3}\text{MnO}_3$ manganites at several temperatures, $f=20$ Hz and $H_{max}=1.35$.

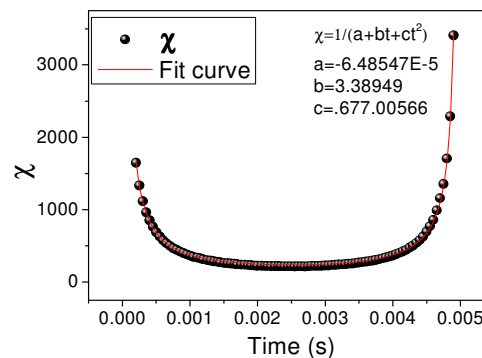


Figure 4. Fit of the AC susceptibility curve as a function of time (t) for $\text{La}_{2/3}\text{Ca}_{1/3}\text{MnO}_3$ manganites at $T=150$ K, $f=20$ Hz and $H_{max}=1.35$.

Figure 2 shows the magnetization for several temperatures as a function of the time, with the frequency being remained constant at $f=20$ Hz. Curves were obtained for temperatures ranging between 100 and 300 K with a step of 2 K. This figure presents a few curves selected to provide a view of the system behavior as the temperature is varied. As is observed, the intensity of the magnetization decreases as the temperature increases. In magnetic systems at low temperatures, the magnetic moments are almost frozen, and therefore, despite the increases in temperature, they are resistant to change their orientation, resulting in a ferromagnetic state [32]. As the temperature increases, the magnetic moments gain energy, increasing their mobility. Next, system entropy appears, producing disorder and decreasing the magnetization [33].

Figure 3 shows several curves of AC susceptibility $\chi(t, T)$ as a function of time for different temperatures obtained using eq. (4). An important characteristic is the strong divergence around the half-way point of the cycle. This divergence produces asymptotic tendencies around the critical point that coincide with the point at which the magnetization changes from positive to negative values. Moreover, at low temperatures, curves are well-defined at both sides of the cycle because the material is in the ferromagnetic phase and is highly ordered. Conversely, as the temperature increases, the points of the curves that are dispersed because of the system reaches the paramagnetic phase that is characterized by a disorder of the spins, as is reflected in the susceptibility curves. Figure 4 presents the susceptibility as a function of time for a temperature $T=150$ K and a frequency of 20 Hz. In this figure, the fit employed to find a , b and c using eq. (5) is presented. This procedure was conducted for each susceptibility curve obtained at all temperatures and frequencies. After the fitting of the susceptibility curves in figure 3 using eq. (3), a Fourier transform is applied employing eq. (7) and (8) to obtain the real and imaginary susceptibility values for the $\text{La}_{2/3}\text{Ca}_{1/3}\text{MnO}_3$ thin films, as is shown in figures 5 (a) and (b), respectively. Both components of the susceptibility decrease as a function of the temperature for several frequencies at a $H_{max}=1.35$ kOe. Two important tendencies were observed in these curves. First, the susceptibility tends to decrease as the temperature increases; both susceptibilities abruptly decrease to zero, exhibiting the ferromagnetic-paramagnetic phase transition [34]. These results are similar to experimental results reported in the literature [35]. A sudden jump is observed, which corresponds to the low temperature ferromagnetic (FM) to paramagnetic (PM) phase transition. For $\text{La}_{2/3}\text{Ca}_{1/3}\text{MnO}_3$, the transition temperature, T_C , has been reported to be approximately 260 K for zero external applied magnetic field (H). Nevertheless, when an external magnetic field is applied, this temperature tends to shift toward higher values, as caused by the order induced by the external magnetic field [3,21,28]. This frequency influence is also observed in these figures. This behavior was

explained by Granado et al [36]. As the frequency increases, the curves of χ'' become less prominent, and the transition shifts to higher temperatures, indicating a transition to a glassy state without long-range magnetic order, such as a spin-glass [37] or a cluster glass state.

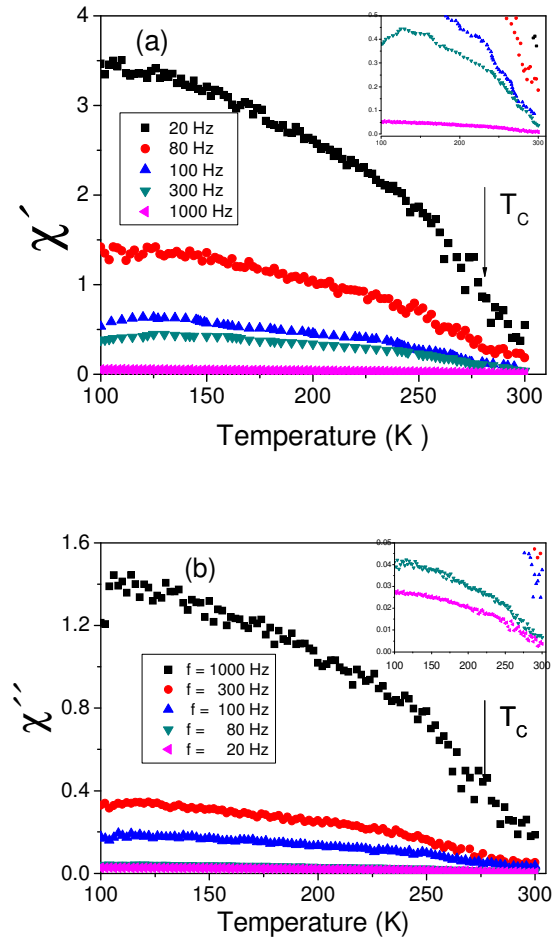


Figure 5. AC susceptibility as a function of temperature for $\text{La}_{2/3}\text{Ca}_{1/3}\text{MnO}_3$ manganites at several frequencies: (a) Real component, χ_n' and (b) imaginary component, χ_n'' . Inset figures represent magnifications of curves for high and low frequencies for χ_n' and χ_n'' , respectively.

IV. CONCLUSIONS

AC magnetic susceptibility was modeled and simulated for $\text{La}_{2/3}\text{Ca}_{1/3}\text{MnO}_3$ manganites using the Heisenberg model, and a Monte Carlo method combined with the Metropolis algorithm. A Fourier transform was used to obtain the real and imaginary components of the susceptibility. The simulations were performed for various frequencies and temperatures. Magnetization curves showed an oscillatory behavior, similar to the external applied magnetic field. The AC magnetic susceptibility was obtained from the magnetization curves as a function of temperature, and the results indicated a transition from ferromagnetic to paramagnetic phases.

AGRADECIMIENTOS

The authors gratefully acknowledge the support of the Departamento de Física y Química of La Universidad Nacional de Colombia Sede Manizales.

REFERENCIAS

- [1] Ramirez A.P., “Colossal magnetoresistance”, *Journal of Physics: Condensed Matter.*, Vol. 9, pp. 8171-8199, 1997.
- [2] Balcells L.L., Fontcuberta J., Martínez B., Obradors X., “High-field magnetoresistance at interfaces in manganese perovskites”, *Physical Review B*, vol. 58, pp. R14697-R14700, 1998.
- [3] Restrepo-Parra E., Bedoya-Hincapie C. M., Orozco-Hernández G., Restrepo J., Jurado J. F., “Monte Carlo Simulation of Magnetotransport Properties $\text{La}_{0.67}\text{Ca}_{0.33}\text{MnO}_3$ (FM) and $\text{La}_{0.33}\text{Ca}_{0.67}\text{MnO}_3$ (AF) Thin Films”, *IEEE Transactions on Magnetics*, vol. 47, pp. 4686-4694, 2011.
- [4] Hejtmánek J., Jiráček Z., Arnold Z., Maryško M., Krupička S., Martin C., Damay F., “Thermal conductivity and magnetic transitions in $\text{Mn}^{3+}/\text{Mn}^{4+}$ manganites”, *Journal of Applied Physics*, vol. 83, pp. 7204-7206, 1998.
- [5] Van Santen J. H., Jonker G. H., “Ferromagnetic compounds of manganese with perovskite structure”, *Physica*, vol. 16, pp. 337-349, 1950.
- [6] Dagotto E., “Nanoscale phase separation and colossal magnetoresistance, the physics of manganites and related compounds”, First ed, Springer-Verlag, New York, 2002.
- [7] Panagiotopoulos I., Christides C., Niarchos D., Pisas M., “Magneto-transport and exchange biasing in La–Ca–Mn–O compositionally modulated ferromagnetic/antiferromagnetic multilayers”, *Journal of Applied Physics*, vol. 87, pp. 3926-3930, 2000.
- [8] Nogués J., Sort J., Langlaib V., Skumryev V., Suriñach S., Muñoz J.S., Baró M.D., “Exchange bias in nanostructures”, *Physics Reports*, vol. 422, pp. 65-117, 2005.
- [9] Giri S., Patra M., Majumdar S., “Exchange bias effect in alloys and compounds”, *Journal of Physics: Condensed Matter*, vol. 23, pp. 1-23, 2011.
- [10] Blasco J., García J., de Teresa J. M., Ibarra M. R., Pérez J., Algarabel P. A., Marquina C., “Structural, magnetic, and transport properties of the giant magnetoresistive perovskites $\text{La}_{2/3}\text{Ca}_{1/3}\text{Mn}_{1-x}\text{Al}_x\text{O}_{3-\delta}$ ”, *Physical Review B*, vol. 55, pp. 8905-8910, 1997.
- [11] Shames A. I., Rozenberg E., Martin C., Maignan A., Raveau B., André G., Gorodetsky G., “Crystallographic structure and magnetic ordering in $\text{CaMn}_{1-x}\text{Ru}_x\text{O}_3$ ($x \leq 0.40$) manganites: Neutron diffraction, ac susceptibility, and electron magnetic resonance studies”, *Physical Review B*, vol. 70, pp. 134433, 2004.
- [12] Chandrasekhar Rao T. V., Raj P., Mohammad Yusur Sk., Madhav Rao L., Sathyamoorthy A., Sahni V. C., “Magnetism in UCu_2Ge_2 : The role of intrinsic domain wall pinning”, *Philosophical Magazine Part B*, vol. 74, pp. 275-291, 1996.
- [13] Kunkel H.P., Williams G., “AC susceptibility of the re-entrant system (PdFe)Mn”, *Journal of Magnetism and Magnetic Materials*, vol. 75, pp. 98-110, 1998.
- [14] Maartense I., Williams G., “ac susceptibility of the ferromagnetic phase of the AuFe system”, *Physical Review B*, vol. 17, pp. 377, 1978.
- [15] Ho S.C., Maartense I., Williams G., “AC susceptibility and resistivity of the ferromagnetic phase of PdMn”, *Journal of Physics F: Metal Physics*, vol. 11, pp. 699-710, 1981.
- [16] Yeshurun Y., Salamon M. B., Rao K. V., Chen H. S., “Critical phenomena in amorphous ferromagnetic and spin-glass alloys”, *Physical Review B*, vol. 24, pp. 1536-1549, 1981.
- [17] Peles A., Kunkel H.P., Zhou X.Z., Williams G., “Field-dependent magnetic and transport properties and anisotropic magnetoresistance in ceramic $\text{La}_{0.67}\text{Pb}_{0.33}\text{MnO}_3$ ”, *Journal of Physics: Condensed Matter*, vol. 11, pp. 8111, 1999.
- [18] Zhao, J. H., Zhou, X. Z., Peles, A., Ge, S. H., Kunkel, H. P., Williams, G., “Indirect evidence for spin-diffusion modes in $\text{La}_{0.67}\text{Ca}_{0.33}\text{MnO}_3$ from field-dependent ac susceptibility measurements”, *Physical Review B: Condensed Matter and Materials Physics*, vol. 59, pp. 8391, 1999.
- [19] Zhao J. H., Kunkel H. P., Zhou X. Z., Williams G., “Magnetic and transport properties, and the phase diagram of hole-doped $\text{La}_{1-x}\text{Mg}_x\text{MnO}_3$ ($x \leq 0.4$)”, *Journal of Physics: Condensed Matter*, vol. 13, pp. 9349, 2001.
- [20] Blasco J., García J., Subías G., M. Sánchez C., “Structure and magnetic properties of $\text{LaMn}_{1-x}\text{Mg}_x\text{O}_3$ compounds”, *Physical Review B*, vol. 70, pp. 094426, 2004.
- [21] Restrepo-Parra E., Bedoya-Hincapie C.M., Jurado F.J., Riano-Rojas J.C., Restrepo J., “Monte Carlo study of the critical behavior and magnetic properties of $\text{La}_{2/3}\text{Ca}_{1/3}\text{MnO}_3$ thin films”, *Journal of Magnetism and Magnetic Materials*, vol. 322, pp. 3514-3518, 2010.
- [22] Şen C., Alvarez G., Dagotto E., “Insulator-to-metal transition induced by disorder in a model for manganites”, *Physical Review B*, vol. 70 pp. 064428, 2004.
- [23] Sengupta P., Sandvik A. W., Singh R. R. P., “Specific heat of quasi-two-dimensional antiferromagnetic Heisenberg models with varying interplanar couplings”, *Physical Review B*, vol. 68, pp. 094423, 2002.
- [24] Panaccione G., Offi F., Sacchi M., Torelli P., “Hard X-ray PhotoEmission Spectroscopy of strongly correlated systems”, *C. R. Physique*, vol. 9, pp. 524-536, 2008.
- [25] Wollan E. O., Koehler W. E., “Neutron Diffraction Study of the Magnetic Properties of the Series of Perovskite-Type Compounds $[(1-x)\text{La}_x\text{Ca}]\text{MnO}_3$ ”, *Physical Review*, vol. 100, pp. 545, 1955.
- [26] Crisan O., Angelakeris M., Flevaris N.K., Sobal N., Giersig M., “Anisotropies in ferromagnetic nanoparticles: simulation and experimental approach”, *Sensors and Actuators A*, vol. 106, pp. 130-133, 2003.
- [27] Hotta T., Feiguin A., Dagotto E., “Stripes induced by orbital ordering in layered manganites”, *Physical Review Letter*, vol. 86, pp. 4922, 2001.

- [28] Riaño-Rojas J.C., Restrepo-Parra E., Orozco-Hernandez G., Restrepo J., Jurado J.F., Vargas-Hernández C., Geometry, “Influence on the Hysteresis Loops Behavior in $\text{La}_{2/3}\text{Ca}_{1/3}\text{MnO}_3$ Nanoparticles. Monte Carlo Simulation on a Heisenberg-Like Model”, *IEEE Transactions on Magnetics*, vol. 45, pp. 5196, 2009.
- [29] Jarner S. F., Hansen E., “Geometric Ergodicity of Metropolis Algorithm”, *Stochastic Processes and their Applications*, vol. 85, pp. 341-361, 2000.
- [30] Cimpoesu D., Stancu A., Spinu L., “Reorientation of magnetic anisotropy in epitaxial cobalt ferrite thin films”, *Physical Review B*, vol. 76, 054409, 2007.
- [31] Trivijitkasem S., Boonchun A., Chantharangsi Ch., Paksunchai Ch., “Analytical study of AC magnetic susceptibility of (Bi, Pb) Sr-Ca-Cu-O superconducting systems using Bean critical state model”, *Kasetsart J. (Nat. Sci.)*, vol. 43, pp. 353–360, 2009.
- [32] Lynn J. W., Erwin R. W., Borchers J. A., Huang Q., Santoro A., Pengand J.-L., Li Z. Y., “Unconventional Ferromagnetic Transition in $\text{La}_{1-x}\text{Ca}_x\text{MnO}_3$ ”, *Physical Review Letter*, vol. 76, pp. 4046-4049, 1996.
- [33] Freericks J. K., Jarrell M., “Magnetic phase diagram of the Hubbard model”, *Physical Review Letters*, vol. 74, pp. 186-189, 1994
- [34] Ramesh Babu M., Han X.F., Ning W., Cheng Z.-h., Sun Y., Jayavel R., “Electron spin resonance and AC susceptibility studies on $\text{La}_{0.9}\text{Pb}_{0.1}\text{MnO}_3$ single crystals”, *Materials Letters*, vol. 63, pp. 1528-1530, 2009.
- [35] Olarte J. A., Mariño A., “EPR and Magnetic Properties on LaCaMnO manganites”, *Momento Revista de Física*, vol. 36, pp. 18-25, 2008.
- [36] Granado R E., Urbano R., Pérez C. A., Azimonte C., Lynn J. W., Souza R. A., Souza-Neto N. M., “Strong orbital correlations in a Fe-substituted spin-glass-manganite”, *Physical Review B*, vol. 72, pp. 052406, 2005.
- [37] Dho J., Kim W. S., Hur N. H., “Reentrant Spin Glass Behavior in Cr-Doped Perovskite Manganite”, *Physical Review Letter*, vol. 89, pp. 027202, 2002.